

pubs.acs.org/synthbio Research Article

# **Engineering Transcriptional Interference through RNA Polymerase Processivity Control**

Nolan J. O'Connor, Antoni E. Bordoy, and Anushree Chatterjee\*



ACCESS

Metrics & More

Article Recommendations

Supporting Information

Tunable TI

Processivity
Control

RNAP

Gene of interest

Inputs
NAND
NOR

NOR

NOR

ABSTRACT: Antisense transcription is widespread in all kingdoms of life and has been shown to influence gene expression through transcriptional interference (TI), a phenomenon in which one transcriptional process negatively influences another *in cis*. The processivity, or uninterrupted transcription, of an RNA polymerase (RNAP) is closely tied to levels of antisense transcription in bacterial genomes, but its influence on TI, while likely important, is not well-characterized. Here, we show that TI can be tuned through processivity control via three distinct antitermination strategies: the antibiotic bicyclomycin, phage protein Psu, and ribosome-RNAP coupling. We apply these methods toward TI and tune ribosome-RNAP coupling to produce 38-fold transcription-level gene repression due to both RNAP collisions and antisense RNA interference. We then couple protein roadblock and TI to design minimal genetic NAND and NOR logic gates. Together, these results show the importance of processivity control for strong TI and demonstrate TI's potential for synthetic biology.

# ■ INTRODUCTION

Antisense transcription is widespread in all kingdoms of life. While once attributed largely to transcriptional noise from hidden or cryptic promoters, antisense transcription is now understood to govern import cellular decisions—for example, meiotic entry in *S. cerevisiae*, senescence effects in fibroblast cells, and antibiotic resistance plasmid conjugation in *E. faecalis*. More recently, high-resolution transcript mapping in bacteria has shown that antisense transcription delineates gene boundaries through bidirectional termination of transcription. Rho-dependent transcriptional termination is understood to suppress antisense transcription in bacteria, but antisense transcription has still been shown to regulate gene expression throughout the genome. Str. No.

There are two known modes of transcriptional regulation by antisense transcription: antisense RNA (asRNA) regulation, where sense and antisense RNAs hybridize to promote RNase-mediated degradation or block the ribosome binding site to prevent its translation, <sup>9–11</sup> and collisions of the transcriptional machinery originated from sense and antisense promoters, termed transcriptional interference (TI). <sup>9,11–13</sup> Three primary modes of TI—RNA Polymerase (RNAP) collisions, sitting

duck, and promoter occlusion—have been proposed<sup>12</sup> and parsed through experiments<sup>14</sup> and mathematical modeling. <sup>10,15</sup> Direct contact of bacterial RNAPs has not been observed during head-on RNAP collisions, <sup>16</sup> and it is thought that interference of one RNAP on another may be mediated through DNA supercoiling <sup>17,18</sup> rather than due to direct collisions of transcriptional machinery. However, in order to maintain consistency with previous TI literature, we use the term "collision" to describe what may be a longer-distance, supercoiling-mediated obstruction of elongating RNAPs, and we depict these collisions as hard contact (Figure 1a). While the mechanism of obstruction is not exactly known, the act of cis-antisense transcription has been shown to reliably downregulate gene expression. <sup>10,14,19–23</sup>

Received: October 21, 2020 Published: March 12, 2021





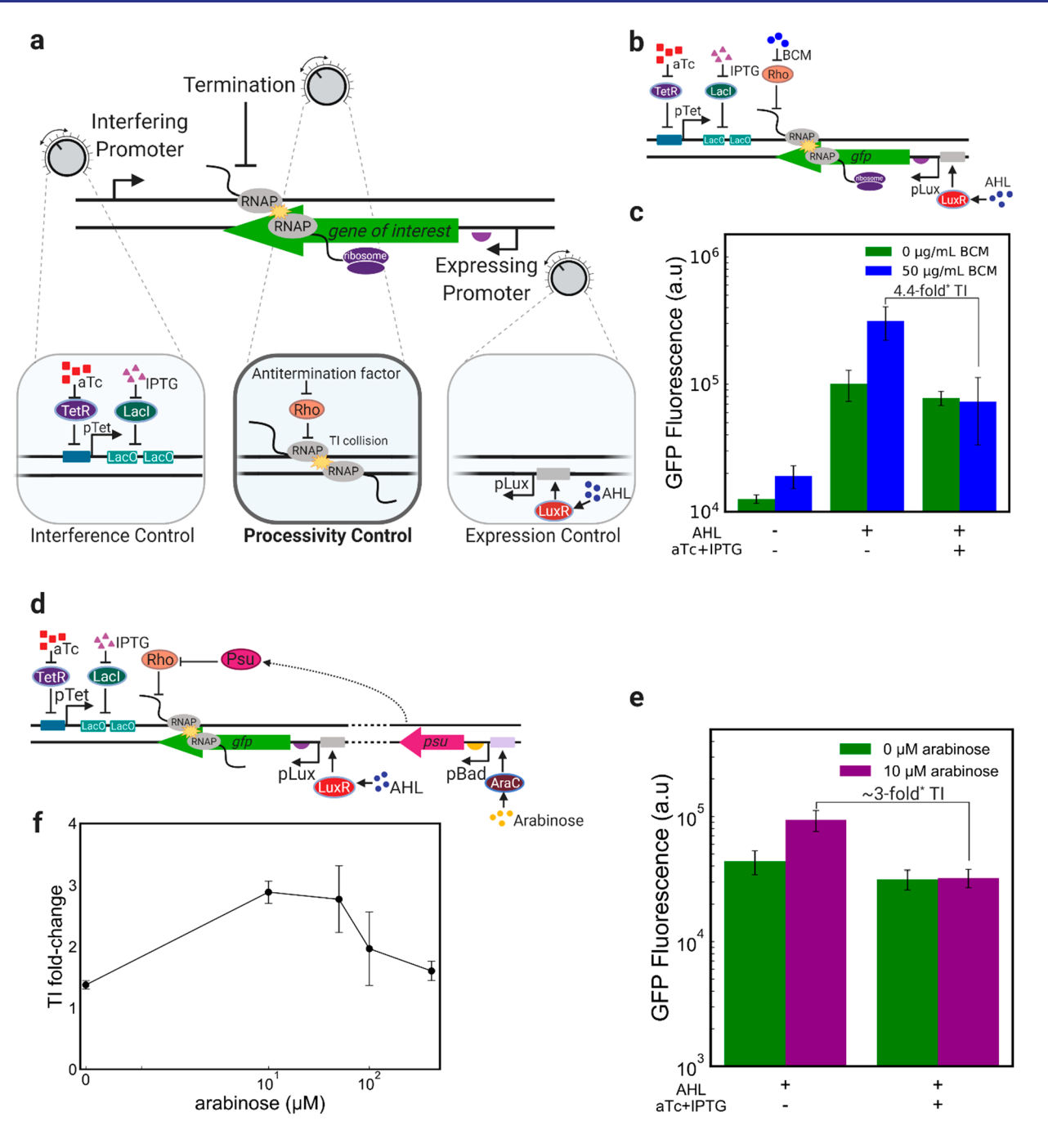


Figure 1. High processivity of interfering RNAPs essential for strong TI. (a) Transcriptional interference (TI) via RNAP collisions is tunable through the expression and interfering promoter strengths and RNAP processivity. Processivity control through antitermination of the interfering RNAP represents a novel strategy to engineer TI. (b) Diagram showing the genetic elements comprising our inducible TI system and illustrating the effects of Rho and its inhibitor antibiotic, bicyclomycin (BCM), on the course of the interfering RNAP. (c) The addition of bicyclomycin (BCM) generates TI through the suppression of Rho termination of the interfering RNAP. (d) Diagram of arabinose-inducible Rho inhibition via Psu. The protein Psu is under the control of the arabinose-inducible pBad promoter. (e) Sublethal Psu expression with 10  $\mu$ M of arabinose creates roughly 3-fold TI. In this experiment, AHL was present at a concentration of 100  $\mu$ M. aTc was present at a concentration of 100 ng/mL, and IPTG was present at a concentration of 1 mM. (f) This construct shows tunable TI, with arabinose activating expression of Psu, which inhibits Rho and thereby improves the processivity of the interfering RNAP and strengthens TI. At high Psu expression, TI is reduced, perhaps due to cell-wide disruption of transcriptional termination. Error bars are denoted as  $\pm$  s.d. Statistical significance as determined through the Mann—Whitney U test (p < 0.05) denoted as \*. n = 3 biological replicates.

While previous TI studies have thoroughly investigated the genetic architectures that influence the frequency of collisions—elements such as interfering and expressing promoter strength<sup>19–21</sup> and interpromoter distance<sup>21</sup>—little attention has been paid to the number of transcription

elongation factors that associate with RNAP during transcription. These proteins—such as NusG, which bridges an RNAP and ribosome during the pioneering round of translation and, in the absence of a cotranslating ribosome, facilitates Rho termination<sup>6,24,25</sup>—affect the processivity, i.e.,

the uninterrupted transcription, of an RNAP. Recent transcriptomic studies in bacteria have linked antisense transcription to Rho termination and the modulation of RNAP processivity, 5-7,26,27 highlighting the importance of RNAP processivity to TI over protein coding sequences. For example, a head-on collision event between an "interfering" RNAP transcribing an untranslated region and an "expressing" RNAP that is coupled to a cotranslating ribosome is likely biased toward the latter due to Rho termination of the former (Figure 1a). Indeed, it was recently shown that an RNAP trailed by a translating ribosome was 13 times more likely to "survive" a head-on RNAP-RNAP collision than an RNAP transcribing untranslated DNA.<sup>22</sup> We hypothesized that protecting interfering RNAPs from Rho termination through processivity control (Figure 1a) could improve the strength of TI and enable its engineering for synthetic biology applications.

Here, we show that engineering processivity control of the interfering RNAP can tune TI. We demonstrate processivity control through the use of three antitermination mechanisms: the antibiotic bicyclomycin, <sup>28</sup> expression of the phage polarity suppression protein Psu, <sup>29–31</sup> and a cotranslating ribosome 22,32,33 improve the strength of RNAP collisions. 22,24,32 We engineer convergent gene constructs that permit an interfering RNAP-ribosome complex ("expressome"34) to enter the opposing gene's open reading frame, causing strong repression of gene expression, and creating, to our knowledge, the first synthetic expressome-on-expressome collision system. We show that processivity control, when coupled with control of interfering and expressing promoters (Figure 1a), creates a layered, tunable TI system. We then apply these design rules to build two-input, minimal NAND and NOR transcriptional logic gates that couple protein roadblock with TI collisions and antisense RNA interference. Together, our results demonstrate the importance of processivity control for tuning and engineering strong TI.

## RESULTS

Processivity Control Is Essential for Strong TI. Transcriptional interference (TI) resulting from convergent promoters can downregulate gene expression of a gene of interest through RNAP collisions and promoter occlusion. The magnitude of this interference depends on the relative strengths of the two promoters 10,19-21 (Figure 1a). Here, we chose to use an inducible promoter system in order to more easily tune their relative strengths. The quorum sensing promoter pLux, induced with AHL, is used as the "expression control" module to regulate gfp production. The aTc-inducible pTet is oriented antisense to gfp and is used as the "interference control" module to downregulate gfp expression through antisense transcription. We added an IPTG-inducible lac operator 47 bp downstream of the pTet transcription start site (Figure 1a) to further tune the interference control via protein roadblock.<sup>35</sup> (DNA lengths for the relevant plasmids are illustrated in Supplementary Figure S1.)

We observed that, when this pTet-LacO architecture (Figure 1b) was activated with saturating aTc and IPTG in order to fire interfering RNAPs to repress GFP expression from pLux, a significant but weak ~1.6-fold change in GFP expression occurred (eq 1, Supplementary Figure S2). We note that pLux exhibits leaky expression and expresses GFP at 0 µM AHL (Supplementary Figure S2). The extent of this TI repression was dependent on both pTet and pLux activity (aTc and AHL concentration, respectively), decreasing with high AHL concentrations and increasing with high aTc concentrations (Supplementary Figure S2). These results demonstrate the effects of interference and expression control on TI and generally agree with other TI studies, which have found that a strong interfering promoter and weak expressing promoter are required to produce significant TI. 19-21

We posited that the weak repression of GFP from TI may be related to low processivity of the interfering RNAP. In vivo, elongating RNAPs interact with transcriptional factors that modulate their processivity.<sup>24</sup> For example, the helicase Rho can translocate along a transcript and terminate transcription.<sup>6,32</sup> Moreover, Rho primarily targets RNAPs transcribing in untranslated regions of DNA in order to suppress pervasive transcription in the genome. 6,22 Because the mRNA transcribed by the interfering RNAP in this construct is not simultaneously being translated, it is susceptible to Rho termination. The RNAPs transcribing gfp are associated with the ribosome through cotranslation (Figure 1b), and since the ribosome has been shown to improve RNAP processivity through reduced Rho termination,<sup>32</sup> there is likely a "bias" in RNAP processivity favoring the expressing promoter. This bias may explain the relatively low levels of observed transcriptional interference (Supplementary Figure S2).

To test this hypothesis, we exposed exponentially growing cells to a sublethal dose of bicyclomycin (BCM), an antibiotic that targets the ATP turnover of Rho, thereby alleviating factor-dependent termination <sup>36</sup> (Figure 1a). The interaction of Rho with BCM provides the "processivity control" in the construct. Upon BCM addition, we observed a significant 4.4fold increase in TI compared to no treatment (Figure 1c), suggesting that Rho inhibition increases interfering RNAP processivity and allows for strong TI. Note that the conditionwide increase in GFP expression in the presence of BCM likely results from decreased termination in the 32 bp 5' UTR region of the expressing promoter.<sup>37</sup> Importantly, the difference in expression between the AHL-only and AHL+aTc+IPTG (Figure 1c) indicates an improvement in interference for RNAPs originating from pTet. These results suggest that the extent of TI can be tuned through control of RNAP processivity.

Phage Polarity Suppression Protein Psu Tunes Tl. The manipulation of RNAP processivity using BCM suggested that the strength of RNAP collisions can be controlled through inhibition of Rho activity. To further fine-tune Rho inibition, we incorporated the P4 phage protein Psu into our plasmid, under a pBad promoter (Supplementary Figure S1, Figure 1d). Similar to BCM, Psu prevents Rho from translocating along the nascent mRNA through inhibition of ATP hydrolysis<sup>29</sup> and has previously been shown to improve RNAP processivity in E. coli.31 To our knowledge, Psu has never before been used to study TI. To reduce crosstalk between IPTG-inducible LacO and arabinose-inducible pBad, we used an araC mutant evolved to respond only to arabinose.<sup>38</sup>

We found that, like BCM, arabinose-induced Psu expression both increases GFP expression and increases the fold-change in TI here to nearly 3-fold (Figure 1e). We also found that induction of Psu with arabinose changed the extent of TI in a dose-dependent manner (Figure 1f), representing a tunable TI system. Interestingly, high levels of Psu induction decreased the observed levels of TI, possibly due to large overall increases in protein expression and promoter leakiness, or a global disruption in gene expression (Supplementary Figure S3). We found that toxicity of Psu expression was neglible if Psu

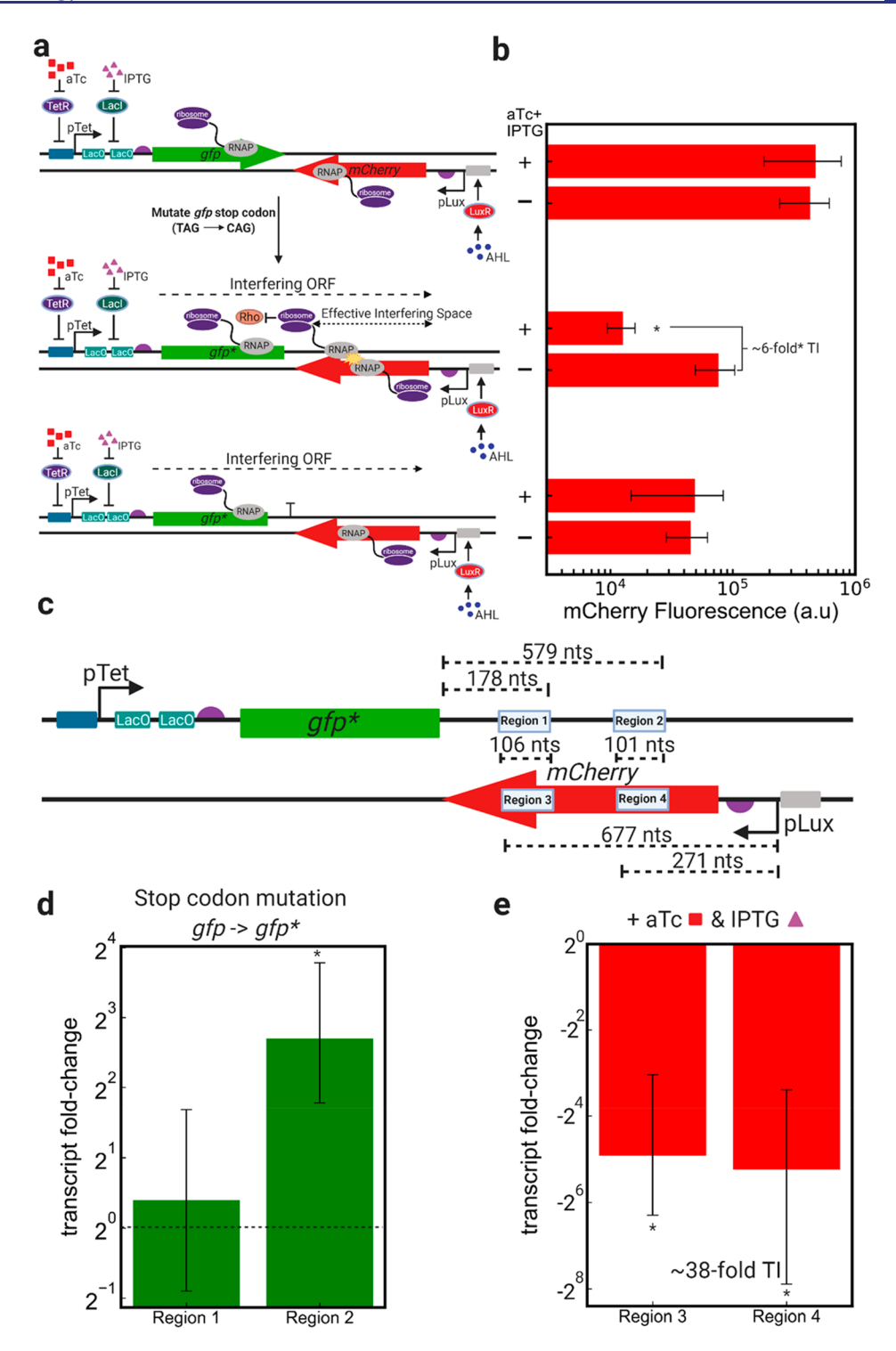


Figure 2. Protecting the interfering RNAP in an expressome complex improves processivity and creates strong TI. (a) Designs of convergent gfp-mCherry constructs: (from top to bottom) convergent gfp and mCherry genes under the control of pTet+LacO and pLux, respectively; convergent gfp and mCherry genes with the gfp stop codon mutated to a glutamine (Gln) amino acid (denoted as gfp\*), thereby extending the ORF originating from downstream of the pTet-LacO 5′-UTR through the mCherry ORF until 2 bp before the pLux transcription start site; a strong unidirectional terminator was inserted downstream of gfp\* to impede the progress of the interfering expressome. (b) mCherry expression with 120 μM AHL and with and without 100 ng/mL aTc and 1 mM IPTG demonstrates the effects of TI on mCherry expression in all constructs. (c) Strand-specific qPCR was used to target transcripts containing regions of the antisense (regions 1 and 2) and sense (regions 3 and 4) mCherry transcripts. Regions 1 and 3 and regions 2 and 4 represent the same amplicons, of sizes 106 and 101 nts, respectively, with different gene-specific cDNA priming (Materials and Methods). (d) Measuring antisense mCherry transcript fold-change (using Kan as a reference) upon gfp stop codon mutation (comparing gfp-mCherry to gfp\*-mCherry) shows improved processivity (increase in region 2 transcripts) upon ribosome–RNAP coupling. Cells containing both constructs were grown in the absence of any AHL (no pLux activation) and in the presence of 100 ng/mL aTc and 1 mM IPTG, in order to measure processivity of the interfering RNAP. Data titled "Region 1" and "Region 2" represent transcripts that contain those amplicon regions (Materials and Methods). (e) Measuring sense mCherry transcript fold-change (using Kan as a reference) upon interfering promoter

Figure 2. continued

activation (comparing AHL-only condition to AHL with aTc+IPTG) shows ~38-fold TI (decrease in regions 3 and 4 transcripts) upon interfering promoter activation. Cells containing both constructs were grown with 200  $\mu$ M AHL (full pLux activation) and in the presence or absence of 100 ng/mL aTc and 1 mM IPTG in order to measure knockdown of the *mCherry* transcript due to TI. Fold-change represents a reduction in transcript levels upon the activation of the interfering promoter, pTet, with aTc and IPTG. Data titled "Region 3" and "Region 4" represent transcripts that contain those amplicon regions (Materials and Methods). For parts d and e, fold change represents changes in transcript levels ( $2^{-\Delta\Delta CT}$ ) upon either mutation of the stop codon (d) or induction of the interfering promoter (e). Error bars are denoted as  $\pm$  s.d, in d and e represented as ( $2^{-(\Delta\Delta CT+s.d)}$ ,  $2^{-(\Delta\Delta CT-s.d)}$ ). \* indicates significance (Mann–Whitney U-test (b), one-sample t test (d,e), p < 0.05) in the expression differences of induced vs uninduced interfering promoter (b) or of the  $\Delta\Delta C_T$  values with respect the null-hypothesis of  $\Delta\Delta C_T$  = 0; d,e). n = 3 biological replicates.

expression was induced after 2 h of growth under orbital shaking (OD of  $\sim$ 0.3; Supplementary Figure S4). Growth effects were, however, observed when arabinose was added upon dilution from overnights, at t=0 (Materials and Methods). We note that the TI fold-change metric used here, in which the AHL-only condition is compared with the AHL+aTc+IPTG condition (eq 1), effectively normalizes any unforeseen effects that may result from cell-wide Rho inhibition.

Both BCM and Psu have previously been shown to increase transcript production for genes that were susceptible to Rhodependent termination while leaving protein levels unchanged, likely due to exclusion of the ribosome<sup>31</sup> resulting from BCM or Psu locking Rho in place on the transcript.<sup>30</sup> The observed increase in fluorescence in our system could be dependent on the 5' UTR of the fluorescent reporter, as a change in length and sequence in this region may reduce interference between Rho and the ribosome.

Ribosomal Protection of the Interfering RNAP Enhances TI over a Gene of Interest. The use of BCM and Psu disrupts Rho termination throughout the cell, limiting their applicability as processivity control strategies. We therefore sought a way to control RNAP processivity in only a gene of interest. The ribosome, when coupled with a transcribing RNAP, protects that RNAP from Rho termination, either through blockage of rho utilization sites or by sequestering NusG through interactions with the NusG CTD and S10 ribosomal subunit.6 Recently, direct and NusGbridged interactions of a bacterial RNAP and ribosome have also been reported and termed the "expressome." 34,39 It has been shown that cotranslation of ribosomes along with elongating RNAPs can prevent the premature termination of the latter by precluding Rho binding. 22,24,32,33 Protecting the interfering RNAP from Rho termination with a cotranslating ribosome in an expressome complex should therefore strengthen gene repression through TI. To this end, we created a construct of convergently oriented gfp and mCherry sequences under the control of pTet-LacO and pLux, respectively (Figure 2a, top). At high AHL concentrations, the use of saturating aTc and IPTG to initiate RNAPs from pTet-LacO did not significantly change mCherry expression, indicating that elongating RNAPs from pTet-LacO did not interfere with RNAPs originating from pLux (Figure 2b, top). Interestingly, we did observe substantial TI-mediated represson of GFP—not mCherry—as a function of the interfering and expressing promoter strengths (Supplementary Figure S5), which may result from sequence differences between the two fluorescent proteins, either in the form of pause sites or Rho utilization sites.

In this convergent *gfp-mCherry* construct, the interfering RNAP has already decoupled from its cotranslating ribosome

before it transcribes into the mCherry ORF (Figure 2a). This "naked" interfering RNAP is more exposed to Rho termination than the expressome complex, and this decoupling of RNAP and ribosome likely explains the lack of observed TI at high AHL concentrations (Figure 2b, top). We hypothesized that if we could prevent RNAP-ribosome decoupling and allow the expressome entry to the mCherry ORF, the resulting increase in interfering RNAP processivity might strengthen TI repression of mCherry. To test this hypothesis, we mutated the stop codon of *gfp* to extend the open reading frame (ORF) of the interfering expressome into the mCherry ORF (Figure 2a, middle). Note that the notation change of gfp to  $gfp^*$ reflects a complete abolition of GFP expression (Supplementary Figure S6). This point mutation resulted in significant, ~6-fold gene repression (Figure 2b, middle) due to the improved processivity of the interfering RNAP when coupled with a cotranslating ribosome. Interestingly, the mutation of the gfp stop codon created an "interfering ORF" that extended through the antisense mCherry ORF and did not encounter an in-frame stop codon until 2 bp prior to the expressing promoter, pLux. Such a long "effective interfering space" (Figure 2a, middle) likely contributed to the improved strength of ribosome-coupled interfering RNAPs.

To confirm that the observed reduction in *mCherry* upon activation of pTet-LacO was due to TI, we added a strong unidirectional terminator (rrnBT1 $^{40}$ ) on the  $gfp^*$  strand between the  $gfp^*$  and mCherry sequences (Figure 2a, bottom) in order to block interfering expressomes from entering the mCherry ORF. Note that this terminator does not introduce any stop codons into the interfering ORF and therefore maintains the interfering expressome course required for strong repression in this construct (Figure 2b). We observed no significant TI when the interfering pTet-LacO module was induced with saturating aTc and IPTG (Figure 2b, bottom), indicating that interactions between transcriptional machinery are likely responsible for the observed gene repression in the  $gfp^*-mCherry$  construct. These results suggest that ribosome-aided RNAP processivity can create strong TI over a gene of interest.

To confirm that the gfp stop codon mutation improved RNAP processivity, we used strand-specific quantitative PCR (qPCR, Materials and Methods) to measure the abundance of transcripts antisense to mCherry in constructs with and without a gfp stop codon (Figure 2c). Under saturation of aTc and IPTG and with no AHL, we measured the relative amounts of transcripts that were long enough to contain regions 1 and 2, located 178 and 579 nts from the 3' end of gfp or  $gfp^*$ , respectively. These data showed that mutating the gfp stop codon does not significantly change the abundance of transcripts long enough to contain region 1 but does significantly change the abundance of transcripts containing

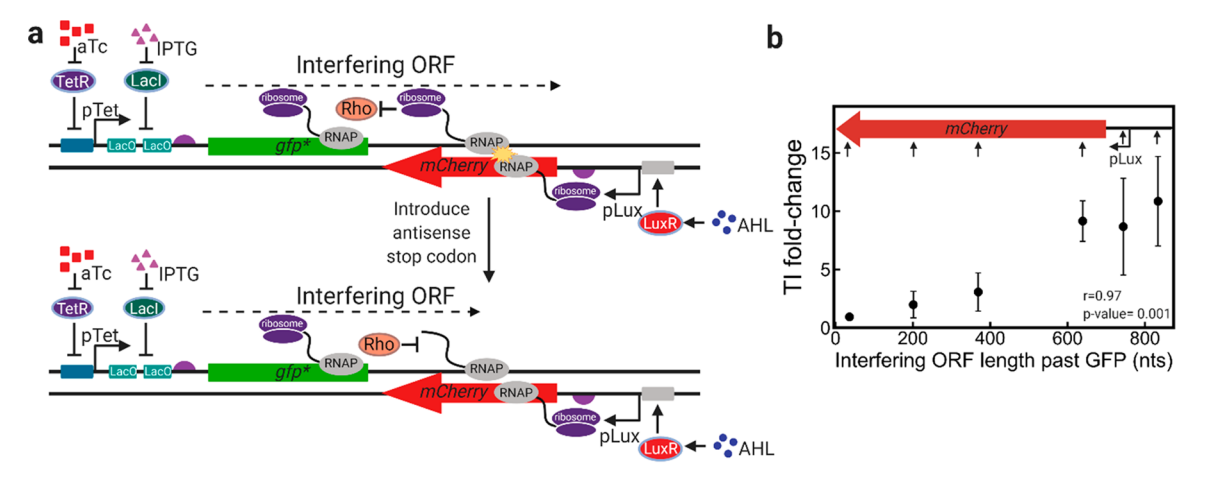


**Figure 3.** TI from a ribosome-protected interfering RNAP is tunable. Using codon degeneracy, stop codons were introduced in the mCherry antisense sequence, maintaining the mCherry amino acid sequence. (a) An example illustrating how these stop codon-introducing point mutations shorten the "interfering ORF" of the interfering expressome. When the interfering ORF is shorter, Rho has a higher chance of terminating transcription of the interfering RNAP and reducing the amount of observed TI. (b) Measuring TI for each construct at identical AHL, aTc, and IPTG concentrations, a trend emerges in which the length of the ORF starting from the start codon of  $gfp^*$  within the mCherry gene dictates the extent of TI. The significant (p value < 0.05) Pearson correlation coefficient suggests a positive relationship between interfering ORF length and TI fold-change. The inserted pLux−mCherry region at the top of the figure shows the positions of the stop codons (represented here as upward arrows) introduced into the antisense strand. The x axis denotes how many nts the interfering expressome will read before encountering a stop codon. Error bars are denoted as  $\pm$  s.d. with  $n \ge 4$  biological replicates.

region 2, at a 6.5-fold increase (Figure 2d). This increase in long antisense transcripts provides transcription-level evidence that the *gfp* stop codon mutation (Figure 2a) improves processivity of the interfering RNAP, as the interfering RNAP, when coupled to a ribosome, is able to transcribe further into the *mCherry* ORF on the antisense strand. This suggests that the TI observed measuring mCherry protein levels (Figure 2b) can be attributed to improved interfering RNAP processivity.

The TI resulting from this improved processivity of the interfering RNAP is also evident when measuring levels of the mCherry transcript. Measuring the relative abundance of the mCherry transcript with saturating AHL and in the presence and absence of interfering promoter induction (with saturating aTc and IPTG) demonstrates a significant, ~38-fold knockdown of the mCherry transcript due to TI (Figure 2e). Amplicons on the 5' and 3' ends of the mCherry transcript, regions 3 and 4 (Figure 2c), were uniformly downregulated upon induction of the interfering promoter. Interestingly, in both the presence and absence of interfering promoter induction, there are ~13-fold more transcripts containing only region 3 than there are transcripts containing regions 3 and 4 (Supplementary Figure S7). This suggests that a number of truncated mCherry transcripts are produced in the gfp\*mCherry construct independent of TI. Both regions are downregulated upon interfering promoter induction, suggesting TI-induced knockdown, but the ratio between the abundances of each transcript length is maintained (Supplementary Figure S7). Premature transcriptional termination has been reported and is a function of the 5' UTR sequence and secondary structure and RBS strength.<sup>31</sup> It is surprising, though, that TI does not affect the relative amounts of truncated transcripts, given that TI is known to create truncated transcripts. <sup>4</sup> This result suggests that TI collisions occur upstream of region 3, toward pLux, or that TI produces truncated mCherry transcripts that maintain the ~13-fold difference between short and long mRNA. We note that the difference in TI fold change when measuring mCherry transcripts using qPCR and mCherry fluorescence using

FACS may be due to the relative half-lives of *mCherry* transcript and protein and the sensitivity of the two assays.

TI from Ribosome-RNAP Coupling Is Tunable through Promoter Control. Previous TI studies have shown that the gene repression due to RNAP collisions is a function of promoter strength. 20-22 Likewise, here we find that TI in this ribosome-aided system can also be tuned through the activation of both expressing (pLux) and interfering (pTet) promoters (Supplementary Figure S8), demonstrating a layered response to processivity, expression, and interference control (Figure 1a). Previous TI studies have demonstrated an inverse relationship between activating promoter strength and TI, 20-22 but interestingly here we observed TI fold-change the ratio of fluorescence observed when the interfering promoter is induced vs uninduced (see Materials and Methods, eq 1)—unchanged for AHL concentrations greater than 20 uM (Supplementary Figure S9). In the absence of a LacI roadblock (at 1 mM IPTG), increasing aTc concentrations reduce mCherry expression due to RNAP collisions, even at high AHL concentrations (Supplementary Figure S8). The aTc-dependence and the dependence of ribosome cotranslation on TI fold change demonstrates the importance of collision location: RNAP collisions must occur over the mCherry ORF—an "effective interfering space" (Figure 2a, middle)—in order to result in observable interference in this system. The coupled effects of strong interfering promoter strength (high aTc) and interfering RNAP processivity (ribosome-RNAP coupling) enable strong TI.

TI Strength Is a Function of the Interfering Expressome's ORF Length. The strong TI observed when the interfering expressome is allowed to read far into the mCherry ORF (Figure 2a-b, middle; Figure 2d), when contrasted with the absence of TI when the interfering expressome encountered a stop codon at the end of gfp (Figure 2a,b, top; Figure 2d), suggests importance to the length of the interfering ORF. Because the likelihood of termination increases after the interfering RNAP decouples from the translating ribosome, 22 the effect of TI should be

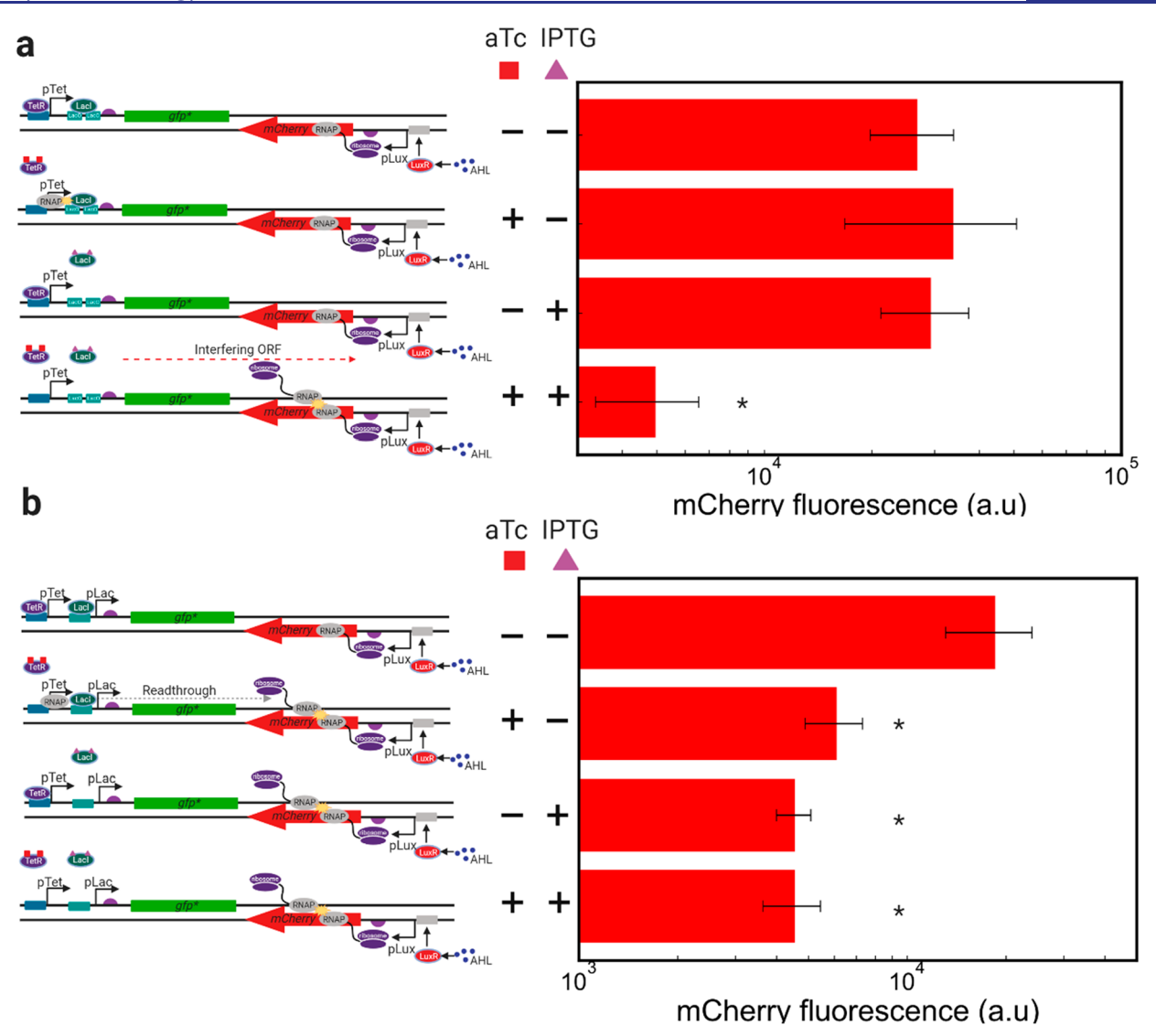


Figure 4. NAND and NOR behaviors arise from coupled roadblock and collisions. Inverting the orientation of a gene of interest in an AND or OR gate creates NAND and NOR logic via TI collisions. (a) Using AND logic with an inducible pTet promoter and LacO operator to control the release of interfering expressomes to collide an interfere mCherry expression creates NAND logic behavior. mCherry expression is plotted with (i) no inducer, (ii) saturating aTc only, (iii) saturating IPTG only, and (iv) saturating aTc + IPTG, revealing NAND behavior for this construct. (b) Using OR logic with a tandem pTet and pLac promoter system generates NOR logic behavior. mCherry expression is plotted with (i) no inducer, (ii) saturating aTc only, (iii) saturating IPTG only, and (iv) saturating aTc + IPTG, revealing NOR behavior for this construct. \* denotes statistical significance compared to the "ON" condition (p < 0.05, Mann—Whitney U test, with n > 3 replicates.).

stronger the longer the interfering RNAP and ribosome can stay coupled.

We tested this hypothesis by introducing stop codons into the antisense *mCherry* sequence, using codon degeneracy to retain the mCherry amino acid sequence (Figure 3a, Supplementary Table S3). These stop codons effectively changed the length of effective interfering space from 744 nts (distance from end of gfp\* to stop codon, for the construct shown in Figure 2) down to lengths of 36, 201, 369, and 639 nts, and up to 834 nts. Transcription and translation therefore uncoupled at different points along the mCherry ORF (Figure 3a). The positive correlation between interfering ORF length and TI fold-change (Pearson correlation coefficient = 0.97, p value <0.05) shows that the location of this uncoupling influences the extent of TI (Figure 3b, right), with early stop codons introduced into the *mCherry* antisense sequence nearly abolishing TI and stop codons downstream of pLux achieving

 $\sim$ 10-fold TI. This result also demonstrates that processivity control through RNAP-ribosome coupling is tunable. Notably, there was barely a trend in TI when the interfering ORF extended past the *mCherry* sequence, at approximately 700 nts, suggesting that pLux promoter occlusion was minimal here. This result agrees with previous mathematical modeling studies,  $^{10,14}$  showing that RNAP collision is the dominant form of TI over large intergenic regions.

Antisense RNA Interference Contributes to mCherry Repression. Reductions in gene expression due to convergently oriented promoters are composed of both collisions of transcriptional machinery and interactions of sense and antisense RNA. Previous studies have knocked out promoters to prevent collisions of transcriptional machinery on the same strand and have found, in some cases significant asRNA interference. In To test the contributions of RNA interference, we designed a

construct that contains two copies of the gfp\*-mCherry transcriptional unit, with the sense and antisense transcription under the control of pLux and pTet-LacO, respectively (Supplementary Figure S10a, right). The transcriptional units are separated and arranged in order to preclude any potential head-on RNAP collisions. We find, upon induction with AHL only and AHL with saturating aTc and IPTG, that mCherry expression is reduced ~2-fold (Supplementary Figure S10a), indicating that asRNA interference works alongside RNAP collisions to downregulate gene expression. We also find, in a different construct (Supplementary Figure S10b, right), that the expression of antisense gfp-mCherry RNA did not cause a reduction in mCherry expression (Supplementary Figure S10b, left). This suggests that the gfp stop codon mutation (gfp  $\rightarrow$ *gfp\**) that improved interfering RNAP processivity (Figure 2d) also enabled antisense RNA interference of mCherry, likely as a result of the longer  $gfp^*-mCherry$  antisense transcripts that contain antisense mCherry and are capable of interfering with mCherry expression.

The ~2-fold difference in mCherry expression from simultaneous transcription of these two gfp\*-mCherry transcriptional units (Supplementary Figure S10a) indicates that some of the ~6-fold reduction in mCherry expression observed in the convergent  $gfp^*$ -mCherry construct (Figure 2b) can be attributed to asRNA interference. We note, however, that although the two transcriptional units in the asRNA interference construct (Supplementary Figure S10) are separated, they do appear to exert some long-distance effects on mCherry expression. In the absence of AHL, aTc and IPTG addition, which drive expression of the interfering asRNA, significantly activate mCherry (Supplementary Figure S10a), potentially due to long-distance RNAP supercoiling-mediated effects<sup>41</sup> and the leakiness of pLux. However, these data demonstrate that here TI and asRNA work in tandem to repress mCherry expression and are aided by improved processivity of the interfering RNAP.

Ribosome-Protected TI and Roadblock Together Can Produce NAND/NOR Logic Behaviors. We next sought to apply processivity control to engineer TI. A handful of prior studies have applied TI to create single-input logic gates,<sup>20</sup> tuning of genetic switches,<sup>19,20</sup> and positive selection systems,<sup>21</sup> and most recently control of metabolism genes in the E. coli genome. 42,43 Given that gene regulation via TI uses a low genetic footprint and requires fewer cellular resources compared with CRISPR interference systems, TI-based genetic devices may be advantageous to the design of larger, more complex genetic programs.<sup>35</sup> Further, coupling processivity control with interference and expression control (Figure 1a) produces a layered response with several "knobs" to tune or adjust the strength or behavior of a TI-based circuit. We therefore proposed that TI with processivity control could be used to design higher-order genetic circuits, such as two-input logic gates.

Roadblocking proteins induce RNAP pausing and act as obstacles to the transcription elongation complex.  $^{35,44}$  We recently demonstrated that TI from an inducible promoter upstream of an inducible roadblock can be rationally engineered to produce AND logic behavior responsive to two chemical inducers, aTc and IPTG.  $^{35}$  We also demonstrated that replacing this roadblock with an inducible promoter creates OR logic behavior after increasing the  $K_{\rm D}$  of the LacI roadblock in order to allow some readthrough from the upstream promoter while lowering leaky expression from

pLac. It follows then that the logic modules used to express AND and OR-like behaviors can be used to control the release of RNAPs that represses GFP expression through RNAP collisions, effectively inverting the logic from AND/OR to NOT AND/OR, i.e., NAND/NOR.

To create NAND behavior, we used the inducible promoter pTet and dowstream protein roadblock LacI to control the release of interfering RNAPs that suppress mCherry expression through collisions (Figure 4a, left). The release of the RNAPs is governed by a two-input AND logic gate, with aTc and IPTG as the inputs, and the interfering expressomes reduce gene expression through collisions, thereby effectively layering a NOT gate onto an AND gate, yielding NAND logic behavior. Using the  $gfp^*-mCherry$  system for ribosome-protected processivity control, we demonstrate good NAND behavior with a 7.8-fold reduction in gene expression due to collisions and asRNA interference (Figure 4a, right).

To create NOR behavior, we used a tandem promoter system composed of pLac and pTet, which was previously shown to demonstrate OR behavior,  $^{35}$  to the  $gfp^*-mCherry$ system to produce strong collisions that repress mCherry expression (Figure 4b, left). Note that the binding affinity of LacI to the LacO binding sites in the downstream promoter was weakened through point mutations in the LacO sequence in order to increase readthrough of RNAP from the upstream promoter.<sup>35</sup> We observed a significant ~4-fold decrease in mCherry expression when either aTc, IPTG, or both were present (Figure 4b, left) at relatively low AHL concentrations (20  $\mu$ L). We note that at higher AHL concentrations, fold change due to TI increases, but the NOR behavior grows asymmetric, 35,45 as the induction of both pTet and pLac at saturating conditions represses mCherry expression further than when either was individually activated (Supplementary Figure S11). This additive effect of the tandem promoters could be due to increased interfering RNAP firing, cooperative readthrough of the tandem RNAPs,46 and/or reduced promoter clogging.<sup>35,47</sup> Together, these results demonstrate the first use of TI for the engineering of higher-order genetic

#### DISCUSSION

The role of TI in genome-wide regulation and genome organization is still being uncovered. Recently, bacterial transcriptome studies have provided a high resolution picture of the E. coli transcriptome and revealed a close relationship between factor-dependent transcriptional termination and TI. 5,7,27 Here, we applied these lessons toward the design of synthetic constructs in which the processivity of an interfering RNAP is engineered to improve the strength of gene repression through transcriptional collisions. We employed three processivity control strategies—the use of the Rhoinhibiting antibiotic bicyclomycin (Figure 1b,c), the phage polarity suppressing protein Psu (Figure 1d,f), and the cotranslation with the ribosome (Figure 2)—to tune the strength of TI collisions. We demonstrated, on a transcription level, the improved processivity control when expressomes are permitted to enter a convergently oriented ORF (Figure 2d) and the resulting ~38-fold reduction in transcript due to TI (Figure 2e). We showed that changing the expression level of Psu (Figure 1f), changing strengths of interfering and expressing promoters (Supplementary Figure S8), and adjusting the length with which the expressome can interfere (Figure 3b) can further tune TI and provide mechanistic insights into

the role of antitermination in strengthening TI. We found that, in agreement with other studies, \$^{10,20,22}\$ asRNA interference likely contributes to down regulation through convergent transcription and is aided by increased processivity of the RNAP transcribing the antisense transcript (Supplementary Figure S10). We then coupled two modes of TI—roadblock and collisions/asRNA interference—to create two-input minimal NAND and NOR logic gates (Figure 4a,b), representing the first functionally complete Boolean gates constructed using TI. Taken together, these results add processivity control as another "tuning knob" for designing TI systems for synthetic biology and expand TI's potential for synthetic biology.

More broadly, these results further emphasize the close connection between RNAP processivity and TI in the genome. Bacteria manipulate RNAP processivity through several different antitermination mechanisms 48 including RNA aptamers, 26 which were recently found to curb levels of antisense transcription and TI throughout the E. coli genome.<sup>2</sup> This suggests an evolved strategy to avoid potentially harmful TI. Conversely, the recent discovery that TI is utilized as a widespread bidirectional terminator in E. coli<sup>5</sup> raises the interesting prospect that ostensibly destructive collisions between RNAPs are evolutionarily selected for, and that genomes are in some part organized to utilize RNAP collisions for gene regulation in a small genetic space. A recent report demonstrated that head-on collisions of replisomes and RNAPs increase the evolvability of convergently oriented genes through mutagenesis, 49 suggesting an evolutionary selection for these convergent arrangements. Collisions between RNAPs, too, could be useful under certain circumstances. It was recently observed that a "noncontiguous operon" governing menaquinone synthesis in S. aureus uses antisense transcription to selectively downregulate gene expression to express drug-tolerant small-colony phenotypes.<sup>5</sup> These findings have stirred interest in TI as a mechanism shaping evolution. Extending the results of this study to the bacterial genome, it seems that the cell's ability to alter the processivity of an RNAP through Rho-dependent transcriptional termination suggests that TI in the genome is potentially "tunable." Indeed, several laboratory adaptation studies for different organisms under different stresses 51-53 have found common Rho and RNAP mutations, suggesting a potential role for TI in bacterial stress responses.

If genomes are arranged to facilitate collisions for regulation, could synthetic circuits also take on such an organization? Here, we sought to expand TI's potential for building genetic devices by engineering processive interfering RNAPs and introducing three distinct methods for processivity control. We note that some synthetic biology applications may require gene knockdowns higher than the 38-fold and 10-fold changes in transcript and protein, respectively, reported here. We postulate that further engineering this system can increase the strength of TI—particularly the leaky expressing promoter, pLux, the dynamics of promoter induction, and the modification of the interfering expressome's RBS<sup>54</sup> to tune to ensure strong transcription-translation coupling. TI systems are capable of ~100-fold changes in gene expression, 20,42 but performance has been shown to depend on gene architecture, promoter strengths, and terminator strengths. 10,19-22 Optimization of these parts, in concert with the processivity control strategy detailed here, should further expand TI's potential for synthetic biology.

Recently, TI has been applied to dynamic control for metabolic engineering. Krylov and colleagues demonstrated the use of an "actuator" sequence element consisting of an antisense promoter, antitermination sequence to protect the antisense RNAPs from Rho termination, and an RNase III processing sequence used to downregulate expression of three *E. coli* metabolism genes. Additionally, Liu and colleagues integrated a TI-based genetic circuit for pyruvate-responsive dynamic control of the central carbon metabolism in *B. subtilis*, resulting in high glucaric acid production. Downregulation of a gene through TI occurs in *cis* and requires fewer resources than CRISPR interference and may improve coordinated knockdown compared with *trans*-encoded sRNA interference, which may benefit metabolic engineering.

Despite notable recent works, TI is still largely understudied, and the "rules" determining where, when, and how RNAPs and/or the expressomes collide are not well understood. Rates of transcription and translation both in the genome and on plasmids are highly context-dependent and depend on the position in an operon and proximity to other genes or genetic elements. Moreover, the role of supercoiling in mediating TI collisions is not well understood but is likely important in determining the strength and location of RNAP collisions in the genome. The coupling of transcription and translation may also enhance supercoiling as the expressome complex cannot easily rotate around DNA. This effect may work in concert with processivity to influence TI. Fundamental insights into these "road rules" of RNAP traffic on the DNA and the resulting TI will reveal how these molecular transcriptional events shape cell physiology and evolution.

#### MATERIALS AND METHODS

Plasmids. Constructs containing fluorescent modules were cloned into pZE21MCS (Expressys) through restriction enzyme cloning and Gibson Assembly. SalI and BamHI were used for the insertion of GFP. GFP was obtained from pAKgfp1 (Addgene #14076). mCherry was obtained from PFPV-mCherry (Addgene #20956). BamHI and MluI were used to invert GFP for NAND and NOR constructs. ApaI was used to insert LuxR. NotI and AgeI were used to insert pLux. All restriction enzymes were purchased from Thermo Fisher. Insertion of psu was performed using a single-enzyme PciI digestion with FastAP. pBad promoters with araC were sourced from pX2\_Cas9 and inserted using Gibson assembly. Primers for Gibson reactions are available upon request. The plasmid containing Psu, pHL 2067, was generously provided by Dr. Han Lim through Addgene.

Point mutations to introduce stop codons into antisense *mCherry* and create orthogonal araC\* mutants were performed using a Quikchange (Agilent) PCR protocol. Single base-pair mismatches in forward and reverse primers were used in a modified PCR cycle to create mismatches, and DpnI was used to digest any original template.

**Strains and Cell Culture.** Cloning and experiments to show logic behavior using TI with GFP and mCherry were performed in *E. coli* strain DH5 $\alpha$ Z1 (Expressys). Transformation colonies were grown in Luria–Bertani (LB) and agar plates supplemented with kanamycin (50  $\mu$ g/mL).

**GFP and mCherry Induction Assays.** Individual colonies were picked from LB and agar plates supplemented with 50  $\mu$ g/mL of kanamycin and incubated for 16 h at 37 °C under orbital shaking at 200 rpm. Then, the cells were diluted 1:10 into fresh LB media supplemented with 50  $\mu$ g/mL kanamycin.

Induction was performed at various inducer concentrations using anhydrous tetracycline (aTc), isopropyl  $\beta$ -D-1-thiogalactopyranoside (IPTG), and 3-oxo-dodecanoyl-L-homoserine lactone (AHL). AHL powder was dissolved in a solution of 99.99% ethyl acetate and 0.01% glacial acetic acid, aliquoted as needed, and stored long-term at −20 °C. Cells were grown for 6-8 h at 37 °C under shaking in a flat-bottom 96-well plate in a microplate reader (Tecan Genios). Optical density at 590 nm was measured during induction. Following the growth period, the cells were transferred to a V-bottom 96-well plate and pelleted by centrifugation of the plate at 4000 rpm for 5 min at 4 °C. The supernatant was removed by vigorously inverting the plate, and then the pellets were resuspended in 100  $\mu$ L of PBS + 4% formaldehyde and transferred to a flat-bottom plate, which was then stored at 4 °C prior to flow cytometry measurements.

Bicyclomycin (BCM) Treatments. A total of 50 ng/mL bicyclomycin (Santa Cruz Biotechnology) was added along with other inducers (aTc, IPTG, AHL) after 3 h of growth under orbital shaking at 200 rpm in LB + Kan following a 1:10 dilution of overnight cultures grown for 16 h. Cells were grown for an additional 3 h before being washed and fixed in PBS + 4% formaldehyde and subsequently measured with flow cytometry.

Psu Experiments. To mitigate the adverse growth effects of high Psu expression, inducers were added to microplate wells (to achieve a total volume of  $100~\mu\text{L}$ ) after 2 h of growth under orbital shaking at 200 rpm in LB + Kan following a 1:10 dilution of overnight cultures grown for 16 h. Cells were grown for an additional 4 h before being washed and fixed in PBS + 4% formaldehyde and subsequently measured with flow cytometry.

**Flow Cytometry.** Before fluorescence measurements conducted with a FACSCelesta instrument, samples were diluted 1:50 in PBS. The 588B 530/30 V (800 V) channel was used to measure GFP levels. FSC-V = 420 V, SSC-V = 260 V, FSC-Threshold = 8000, and SSC-Threshold = 200. For each sample, 50,000 cells were measured. At least four biological replicates were collected for each construct. Data were analyzed using the FlowCytometryTools package in Python 3.7. Statistical differences were examined using the Mann—Whitney U test.

To calculate the TI fold-change for a particular construct or set of conditions, mean fluorescence values of biological replicates (minimum 3) were averaged and used in the following equation:

$$TI fold change = \frac{Fluorescence_{AHLonly}}{Fluorescence_{AHL+aTc+IPTG}}$$
(1)

**Strand-Specific qPCR.** Growth Experiment and RNA Isolation. One-milliliter overnights in LB media supplemented with 50  $\mu$ g/mL kanamycin were grown for at 37 °C under orbital shaking for 16 h. Overnight cultures were diluted 1:50 into LB media with 50  $\mu$ g/mL kanamycin and relevant inducers (aTc, IPTG, AHL) and grown for 6 h at 37 °C with orbital shaking at a total volume of 1.5 mL. Cell pellets were spun down for 2 min at 12000 rcf. The supernatant was removed, and pellets were stored at -80 °C prior to RNA extraction. RNA was extracted and purified using a GeneJET RNA Purification Kit (Thermo Fisher). Total RNA was digested with DNase I at 37 °C for 30 min and subsequently repurified.

cDNA Synthesis. cDNA synthesis was carried out using a High Capacity cDNA Reverse Transcription Kit (Applied Biosystems). Gene-specific primers corresponding to the antisense *mCherry* sequence were used to prime cDNA synthesis. A total of 2  $\mu$ L of primer at 10  $\mu$ M and ~500 ng of RNA were added to the 24  $\mu$ L reaction. cDNA synthesis was carried out using the temperature steps: 25 °C for 10 min; 37 °C for 2 h, 85 °C for 5 min, and a 4 °C hold.

RT-qPCR. RT-qPCR was carried out using FastStart Universal SYBR Green Master Mix (Rox; Sigma-Aldrich) in an Applied Biosystems QuantStudio 6. 1.5  $\mu$ L of cDNA, and 1  $\mu$ L of reverse and forward primers were added to each 10  $\mu$ L reaction. Kanamycin was used as a reference housekeeping gene for each construct. Threshold values were normalized to Kan ( $\Delta$ C<sub>T</sub>), and these  $\Delta$ C<sub>T</sub> values for gfp-mCherry and gfp\*-mCherry (Figure 2d) or no aTc+IPTG and aTc+IPTG (Figure 2e) were compared ( $\Delta$ \DeltaC<sub>T</sub>). Error from biological replicates was propagated through normalization and comparisons. Fold-change error bounds are reported as  $2^{-(\Delta\Delta$ CT+sd)} and  $2^{-(\Delta\Delta$ CT-sd)} calculated comparing the CT values for gfp-mCherry and gfp\*-mCherry (Figure 2d) or no aTc+IPTG to 100 ng/mL aTc + 1 mM IPTG (Figure 2e).

#### ASSOCIATED CONTENT

# Supporting Information

The Supporting Information is available free of charge at https://pubs.acs.org/doi/10.1021/acssynbio.0c00534.

Supplementary Tables S1-S3, Supplementary Figures S1-S11, and Supplemental References (PDF)

#### AUTHOR INFORMATION

### **Corresponding Author**

Anushree Chatterjee — Department of Chemical and Biological Engineering, University of Colorado Boulder, Boulder, Colorado 80303, United States; Antimicrobial Regeneration Consortium, Boulder, Colorado 80301, United States; Sachi Bioworks, Inc., Boulder, Colorado 80301, United States; orcid.org/0000-0002-8389-9917; Email: chatterjee@colorado.edu

# **Authors**

Nolan J. O'Connor – Department of Chemical and Biological Engineering, University of Colorado Boulder, Boulder, Colorado 80303, United States

Antoni E. Bordoy — Department of Chemical and Biological Engineering, University of Colorado Boulder, Boulder, Colorado 80303, United States

Complete contact information is available at: https://pubs.acs.org/10.1021/acssynbio.0c00534

#### **Author Contributions**

N.J.O, A.E.B, and A.C designed the study. N.J.O performed the experiments and analyzed the data. N.J.O and A.C wrote the paper.

# **Funding**

National Science Foundation Grant No. MCB1714564 to A.C.

The authors declare no competing financial interest.

## ACKNOWLEDGMENTS

The authors wish to acknowledge the GAANN fellowship given to N.J.O. through the Department of Education, the

S10ODO21601 Grant given to the Flow Cytometry Facility of the University of Colorado Boulder, the Next-Gen Sequencing Core at the University of Colorado Boulder, and the National Science Foundation Grant No. MCB1714564 to A.C.

## REFERENCES

- (1) Wade, J. T., and Grainger, D. C. (2014) Pervasive Transcription: Illuminating the Dark Matter of Bacterial Transcriptomes. *Nat. Rev. Microbiol.* 12 (9), 647–653.
- (2) Hongay, C. F., Grisafi, P. L., Galitski, T., and Fink, G. R. (2006) Antisense Transcription Controls Cell Fate in Saccharomyces Cerevisiae. *Cell* 127 (4), 735–745.
- (3) Muniz, L., Deb, M. K., Aguirrebengoa, M., Lazorthes, S., Trouche, D., and Nicolas, E. (2017) Control of Gene Expression in Senescence through Transcriptional Read-Through of Convergent Protein-Coding Genes. *Cell Rep.* 21 (9), 2433–2446.
- (4) Chatterjee, A., Johnson, C. M., Shu, C.-C., Kaznessis, Y. N., Ramkrishna, D., Dunny, G. M., and Hu, W.-S. (2011) Convergent Transcription Confers a Bistable Switch in Enterococcus Faecalis Conjugation. *Proc. Natl. Acad. Sci. U. S. A.* 108 (23), 9721–9726.
- (5) Ju, X., Li, D., and Liu, S. (2019) Full-Length RNA Profiling Reveals Pervasive Bidirectional Transcription Terminators in Bacteria. *Nat. Microbiol.* 4, 1907.
- (6) Peters, J. M., Mooney, R. A., Grass, J. A., Jessen, E. D., Tran, F., and Landick, R. (2012) Rho and NusG Suppress Pervasive Antisense Transcription in Escherichia Coli. *Genes Dev.* 26 (23), 2621–2633.
- (7) Dar, D., and Sorek, R. (2018) High-Resolution RNA 3-Ends Mapping of Bacterial Rho-Dependent Transcripts. *Nucleic Acids Res.* 46 (13), 6797–6805.
- (8) Sedlyarova, N., Shamovsky, I., Bharati, B. K., Epshtein, V., Chen, J., Gottesman, S., Schroeder, R., and Nudler, E. (2016) SRNA-Mediated Control of Transcription Termination in E. Coli. *Cell* 167 (1), 111–121 e13..
- (9) Courtney, C., and Chatterjee, A. (2014) Cis-Antisense RNA and Transcriptional Interference: Coupled Layers of Gene Regulation. *J. Gene Ther* 2 (1), 1–9.
- (10) Bordoy, A. E., and Chatterjee, A. (2015) Cis-Antisense Transcription Gives Rise to Tunable Genetic Switch Behavior: A Mathematical Modeling Approach. *PLoS One 10* (7), No. e0133873.
- (11) Pelechano, V., and Steinmetz, L. M. (2013) Gene Regulation by Antisense Transcription. *Nat. Rev. Genet.* 14 (12), 880–893.
- (12) Shearwin, K. E., Callen, B. P., and Egan, J. B. (2005) Transcriptional Interference A Crash Course. *Trends Genet.* 21 (6), 339–345.
- (13) Georg, J., and Hess, W. R. (2011) Cis-Antisense RNA, Another Level of Gene Regulation in Bacteria. *Microbiol. Mol. Biol. Rev.* 75 (2), 286–300.
- (14) Palmer, A. C., Ahlgren-Berg, A., Egan, J. B., Dodd, I. B., and Shearwin, K. E. (2009) Potent Transcriptional Interference by Pausing of RNA Polymerases over a Downstream Promoter. *Mol. Cell* 34 (5), 545–555.
- (15) Sneppen, K., Dodd, I. B., Shearwin, K. E., Palmer, A. C., Schubert, R. a, Callen, B. P., and Egan, J. B. (2005) A Mathematical Model for Transcriptional Interference by RNA Polymerase Traffic in Escherichia Coli. *J. Mol. Biol.* 346 (2), 399–409.
- (16) Crampton, N., Bonass, W. A., Kirkham, J., Rivetti, C., and Thomson, N. H. (2006) Collision Events between RNA Polymerases in Convergent Transcription Studied by Atomic Force Microscopy. *Nucleic Acids Res.* 34 (19), 5416–5425.
- (17) Meyer, S., and Beslon, G. (2014) Torsion-Mediated Interaction between Adjacent Genes. *PLoS Comput. Biol.* 10 (9), No. e1003785.
- (18) Yeung, E., Dy, A. J., Martin, K. B., Ng, A. H., Del Vecchio, D., Beck, J. L., Collins, J. J., and Murray, R. M. (2017) Biophysical Constraints Arising from Compositional Context in Synthetic Gene Networks. *Cell Syst.* 5 (1), 11–24 e12..
- (19) Bordoy, A. E., Varanasi, U. S., Courtney, C. M., and Chatterjee, A. (2016) Transcriptional Interference in Convergent Promoters as a

- Means for Tunable Gene Expression. ACS Synth. Biol. 5 (12), 1331–1341.
- (20) Brophy, J. A. N., and Voigt, C. A. (2016) Antisense Transcription as a Tool to Tune Gene Expression. *Mol. Syst. Biol.*, 1–14.
- (21) Hoffmann, S. A., Kruse, S. M., and Arndt, K. M. (2016) Long-Range Transcriptional Interference in E. Coli Used to Construct a Dual Positive Selection System for Genetic Switches. *Nucleic Acids Res.* 44 (10), No. gkw125.
- (22) Hoffmann, S. A., Hao, N., Shearwin, K. E., and Arndt, K. M. (2019) Characterizing Transcriptional Interference between Converging Genes in Bacteria. ACS Synth. Biol. 8 (3), 466–473.
- (23) Hao, N., Palmer, A. C., Ahlgren-Berg, A., Shearwin, K. E., and Dodd, I. B. (2016) The Role of Repressor Kinetics in Relief of Transcriptional Interference between Convergent Promoters. *Nucleic Acids Res.*, No. gkw600.
- (24) McGary, K., and Nudler, E. (2013) RNA Polymerase and the Ribosome: The Close Relationship. *Curr. Opin. Microbiol.* 16 (2), 112–117
- (25) Cardinale, C. J., Washburn, R. S., Tadigotla, V. R., Brown, L. M., Gottesman, M. E., and Nudler, E. (2008) Termination Factor Rho and Its. *Science (Washington, DC, U. S.)* 320 (May), 935–938.
- (26) Sedlyarova, N., Rescheneder, P., Magán, A., Popitsch, N., Rziha, N., Bilusic, I., Epshtein, V., Zimmermann, B., Lybecker, M., Sedlyarov, V., et al. (2017) Natural RNA Polymerase Aptamers Regulate Transcription in E. Coli. *Mol. Cell* 67 (1), 30–43 e6..
- (27) Magan, A., Amman, F., El-Isa, F., Hartl, N., Shamovsky, I., Sedlyarova, N., and Nudler, E. (2019) IRAPs Curb Antisense Transcription in E. Coli. *Nucleic Acids Res*. No. 22, 1–12.
- (28) Skordalakes, E., Brogan, A. P., Park, B. S., Kohn, H., and Berger, J. M. (2005) Structural Mechanism of Inhibition of the Rho Transcription Termination Factor by the Antibiotic Bicyclomycin. *Structure* 13 (1), 99–109.
- (29) Pani, B., Banerjee, S., Chalissery, J., Abishek, M., Loganathan, R. M., Suganthan, R. B., and Sen, R. (2006) Mechanism of Inhibition of Rho-Dependent Transcription Termination by Bacteriophage P4 Protein Psu. J. Biol. Chem. 281 (36), 26491–26500.
- (30) Ranjan, A., Banerjee, R., Pani, B., Sen, U., and Sen, R. (2013) The Moonlighting Function of Bacteriophage P4 Capsid Protein, Psu, as a Transcription Antiterminator. *Bacteriophage* 3 (2), No. e25657.
- (31) Hussein, R., Lee, T. Y., and Lim, H. N. (2015) Quantitative Characterization of Gene Regulation by Rho Dependent Transcription Termination. *Biochim. Biophys. Acta, Gene Regul. Mech.* 1849 (8), 940–954.
- (32) Artsimovitch, I. (2018) Rebuilding the Bridge between Transcription and Translation. *Mol. Microbiol.* 108 (5), 467–472.
- (33) Proshkin, S., Rahmouni, A. R., Mironov, A., and Nudler, E. (2010) Cooperation Between Translating Ribosomes and RNA Polymerase in Transcription Elongation. *Science (Washington, DC, U. S.)* 328 (April), 504–508.
- (34) Kohler, R., Mooney, R. A., Mills, D. J., Landick, R., and Cramer, P. (2017) Architecture of a Transcribing-Translating Expressome. *Science* (80-). 356 (6334), 194LP-197.
- (35) Bordoy, A. E., O'Connor, N. J., and Chatterjee, A. (2019) Construction of Two-Input Logic Gates Using Transcriptional Interference. ACS Synth. Biol. 8 (10), 2428–2441.
- (36) Peters, J. M., Mooney, R. A., Kuan, P. F., Rowland, J. L., Keles, S., and Landick, R. (2009) Rho Directs Widespread Termination of Intragenic and Stable RNA Transcription. *Proc. Natl. Acad. Sci. U. S. A.* 106 (36), 15406–15411.
- (37) Hussein, R., Lee, T. Y., and Lim, H. N. (2015) Quantitative Characterization of Gene Regulation by Rho Dependent Transcription Termination. *Biochim. Biophys. Acta, Gene Regul. Mech.* 1849 (8), 940–954.
- (38) Lee, S. K., Chou, H. H., Pfleger, B. F., Newman, J. D., Yoshikuni, Y., and Keasling, J. D. (2007) Directed Evolution of AraC for Improved Compatibility of Arabinose- and Lactose-Inducible Promoters. *Appl. Environ. Microbiol.* 73 (18), 5711–5715.

- (39) Webster, M. W., Takacs, M., Zhu, C., Vidmar, V., Eduljee, A., and Weixlbaumer, A. (2020) Structural basis of transcription-translation coupling and collision in bacteria. *Science* 3, 1355–1359.
- (40) Orosz, A., Boros, I., and Venetianer, P. (1991) Analysis of the Complex Transcription Termination Region of the Escherichia Coli Rrn B Gene. Eur. J. Biochem. 201 (3), 653–659.
- (41) Kim, S., Beltran, B., Irnov, I., and Jacobs-Wagner, C. (2019) Long-Distance Cooperative and Antagonistic RNA Polymerase Dynamics via DNA Supercoiling. *Cell* 179 (1), 106–119 e16.
- (42) Krylov, A. A., Shapovalova, V. V., Miticheva, E. A., Shupletsov, M. S., and Mashko, S. V. (2020) Universal Actuator for Efficient Silencing of Escherichia Coli Genes Based on Convergent Transcription Resistant to Rho-Dependent Termination. ACS Synth. Biol. 9 (7), 1650–1664.
- (43) Xu, X., Li, X., Liu, Y., Zhu, Y., Li, J., Du, G., Chen, J., Ledesma-Amaro, R., and Liu, L. (2020) Pyruvate-Responsive Genetic Circuits for Dynamic Control of Central Metabolism. *Nat. Chem. Biol.* 16, 1261
- (44) Hao, N., Krishna, S., Ahlgren-Berg, A., Cutts, E. E., Shearwin, K. E., and Dodd, I. B. (2014) Road Rules for Traffic on DNA-Systematic Analysis of Transcriptional Roadblocking in Vivo. *Nucleic Acids Res.* 42, 8861–8872.
- (45) Cox, R. S., Surette, M. G., and Elowitz, M. B. (2007) Programming Gene Expression with Combinatorial Promoters. *Mol. Syst. Biol.* 3 (145), 145.
- (46) Epshtein, V., Toulmé, F., Rahmouni, A. R., Borukhov, S., and Nudler, E. (2003) Transcription through the Roadblocks: The Role of RNA Polymerase Cooperation. *EMBO J.* 22 (18), 4719–4727.
- (47) Hao, N., Krishna, S., Ahlgren-Berg, A., Cutts, E. E., Shearwin, K. E., and Dodd, I. B. (2014) Road Rules for Traffic on DNA—Systematic Analysis of Transcriptional Roadblocking in Vivo. *Nucleic Acids Res.* 42 (14), 8861–8872.
- (48) Santangelo, T. J., and Artsimovitch, I. (2011) Termination and Antitermination: RNA Polymerase Runs a Stop Sign. *Nat. Rev. Microbiol.* 9 (5), 319–329.
- (49) Merrikh, C. N., and Merrikh, H. (2018) Gene Inversion Potentiates Bacterial Evolvability and Virulence. *Nat. Commun.* 9 (1), 4662.
- (50) Saenz-Lahoya, S., Bitarte, N., Garcia, B., Burgui, S., Vergara-Irigaray, M., Valle, J., Solano, C., Toledo-Arana, A., and Lasa, I. (2019) Noncontiguous Operon Is a Genetic Organization for Coordinating Bacterial Gene Expression. *Proc. Natl. Acad. Sci. U. S. A. 116* (5), 1733–1738.
- (51) Tenaillon, O., Rodríguez-Verdugo, A., Gaut, R. L., McDonald, P., Bennett, A. F., Long, A. D., and Gaut, B. S. (2012) The Molecular Diverstiy of Adaptive Convergence. *Science (Washington, DC, U. S.)* 335 (6067), 457–462.
- (52) Freddolino, P. L., Goodarzi, H., and Tavazoie, S. (2012) Fitness Landscape Transformation through a Single Amino Acid Change in the Rho Terminator. *PLoS Genet.* 8 (5), e1004940.
- (53) Lee, Y. H., and Helmann, J. D. (2014) Mutations in the Primary Sigma Factor ΣAand Termination Factor Rho That Reduce Susceptibility to Cell Wall Antibiotics. *J. Bacteriol.* 196 (21), 3700–3711.
- (54) Salis, H. M., Mirsky, E. a, and Voigt, C. a. (2009) Automated Design of Synthetic Ribosome Binding Sites to Control Protein Expression. *Nat. Biotechnol.* 27 (10), 946–950.
- (55) Lim, H. N., Lee, Y., and Hussein, R. (2011) Fundamental Relationship between Operon Organization and Gene Expression. *Proc. Natl. Acad. Sci. U. S. A.* 108 (26), 10626–10631.
- (56) Scholz, S. A., Diao, R., Wolfe, M. B., Fivenson, E. M., Lin, X. N., and Freddolino, P. L. (2019) High-Resolution Mapping of the Escherichia Coli Chromosome Reveals Positions of High and Low Transcription. *Cell Syst.* 8 (3), 212–225 e9.
- (57) Liu, L. F., and Wang, J. C. (1987) Supercoiling of the DNA Template during Transcription. *Proc. Natl. Acad. Sci. U. S. A.* 84 (20), 7024–7027.